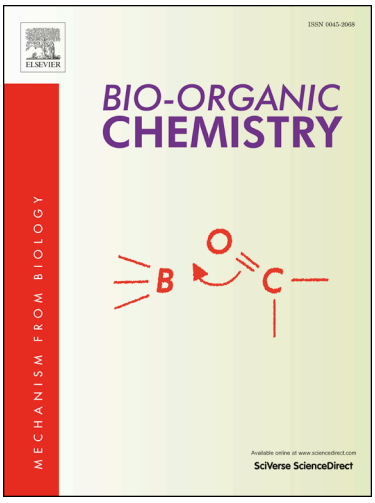

Inhibitory properties of aromatic thiosemicarbazones on mushroom tyrosinase: Synthesis, kinetic studies, molecular docking and effectiveness in melanogenesis inhibition

K. Hałdys, W. Goldeman, M. Jewgiński, E. Wolińska, N. Anger, J. Rossowska, R. Latajka

PII: S0045-2068(18)30591-1
DOI: https://doi.org/10.1016/j.bioorg.2018.09.003
Reference: YBIOO 2500

To appear in: *Bioorganic Chemistry*

Received Date: 15 June 2018
Revised Date: 5 September 2018
Accepted Date: 6 September 2018

Please cite this article as: K. Hałdys, W. Goldeman, M. Jewgiński, E. Wolińska, N. Anger, J. Rossowska, R. Latajka, Inhibitory properties of aromatic thiosemicarbazones on mushroom tyrosinase: Synthesis, kinetic studies, molecular docking and effectiveness in melanogenesis inhibition, *Bioorganic Chemistry* (2018), doi: https://doi.org/10.1016/j.bioorg.2018.09.003

Inhibitory properties of aromatic thiosemicarbazones on mushroom tyrosinase: Synthesis, kinetic studies, molecular docking and effectiveness in melanogenesis inhibition

K. Hałdys[1*], W. Goldeman[2], M. Jewgiński[1], E. Wolińska[1], N. Anger[3], J. Rossowska[3], R. Latajka[1]

[1]Department of Organic and Pharmaceutical Technology, Wrocław University of Science and Technology, Wybrzeże Wyspiańskiego 27, 50-370 Wrocław, Poland
[2]Department of Organic Chemistry, Wrocław University of Science and Technology, Wybrzeże Wyspiańskiego 27, 50-370 Wrocław, Poland
[3]Ludwik Hirszfeld Institute of Immunology and Experimental Therapy, Polish Academy of Science, Rudolfa Weigla 12, 53-114 Wrocław, Poland

Abstract

The group of 19 thiosemicarbazones (TSCs) were synthesized and its inhibitory activity toward mushroom tyrosinase and ability to inhibition of melanogenesis in B16 cells were investigated. Moreover, molecular docking of these compounds to the active site of the enzyme was performed. The obtained results allowed to make the structure-activity relationship (SAR) analysis. Kinetic studies revealed that TSCs 1, 2, 11 and 18 have better inhibitory properties than kojic acid, a reference compound, with the best inhibitory constant (K_i) value of 0,38 µM for TSC 2. According to SAR analysis, the smaller and less branched molecules exhibit higher affinity to the enzyme. Melanin production in B16 cells was inhibited by all investigated compounds at micromolar level. Most of compounds studied in this work can be considered as potent inhibitors of tyrosinase and melanogenesis. They may have broad application in food preservatives and cosmetics. Combined results of molecular docking and SAR analysis can be helpful in designing novel tyrosinase inhibitors of desired properties.

katarzyna.haldys@pwr.edu.pl; waldemar.goldeman@pwr.edu.pl; michal.jewginski@pwr.edu.pl; ewa.mrozinska@pwr.edu.pl; natalia.anger@iitd.pan.wroc.pl; joanna@iitd.pan.wroc.pl; rafal.latajka@pwr.edu.pl

Keywords: tyrosinase, thiosemicarbazones, kinetic studies, SAR, molecular docking, B16F10 cell line.

1. Introduction

Tyrosinase (EC 1.14.18.1) is a type III copper protein with two copper ions in its active site. The enzyme catalyzes the hydroxylation of monophenols to o-diphenols (monophenolase activity) and subsequent oxidation of the o-diphenols to the corresponding o-quinones (diphenolase activity). When L-tyrosine is the substrate, the product of tyrosinase catalyzed reaction is dopaquinone which is then converted to melanins [1].

Melanins are the family of pigments known for their ability to protect the mammalian skin from damage caused by ultraviolet radiation (UV). Melanin absorbs UV sunlight and removes reactive oxygen species (ROS). Melanocytes are special cells within the basal layer of the dermis, secreting the pigment. The amount, type and distribution of melanins in surrounding keratinocytes determines the color of the human skin [2].

Hyperactivity of tyrosinase leads to overproduction of melanin which is accumulated in the skin causing many dermatological disorders. Such hyperpigmentation problems include freckles, melasma, post inflammatory melanoderma, age spots and melanoma [3].

There is a growing trend for lighter skin in the whole world with Asia as the largest skin whitening products market. Around 15% of the world population, including both men and women, buys skin lightening cosmetics. Global Industry Analysts, Inc. predicts that the global market for skin lightening agents will reach US$23 billion by 2020 [4].

Moreover, a lot of disorders in melanin biosynthesis pathway are related to some neurodegenerative diseases, such as, Alzheimer's as well as Parkinson's and Huntington's diseases [5].

Tyrosinase is also responsible for enzymatic browning in plant-derived foods. Formation of brown or black pigment in fruits and vegetables is the main factor affecting the shelf life of fresh-cut products, leading to decreased sensory properties. Browning spoils the senses and taste. Furthermore, some of *o*-quinone compounds can combine with protein residue groups (e.g. amino, sulfhydryl) to change the nutrition characteristics of the protein [6].

Because of their biological and pharmacological properties, aromatic thiosemicarbazones have been recently the compounds of great interest to medicinal chemists. They have been used in antimicrobial [7], antimalarial [8] and anticancer [9,10] treatment.

For the past ten years thiosemicarbazones have been also intensively studied as tyrosinase inhibitors [11-29]. Derivatives of benzaldehyde thiosemicarbazone [11-18], acetophenone thiosemicarbazone [19-21] and aromatic heterocycle thiosemicarbazone [22-28] exhibited potent inhibitory activity.

As they possess thiourea moiety, thiosemicarbazone derivatives are potential donor ligands for transition metal ions [30]. It was reported that thiosemicarbazone derivatives are potent tyrosinase inhibitors because the sulfur and nitrogen atoms of the thiourea moiety are able to chelate copper ions in the active site of tyrosinase [21].

Many potent tyrosinase inhibitors already described in the literature bear phenyl group [31,32] what refers to the natural tyrosinase substrates, L-tyrosine and L-dopa. High affinity of such compounds to the enzyme is the result of the van der Waals interactions of phenyl group with the residues present in the hydrophobic tyrosinase cavity [21].

The aim of the present paper is, to study the inhibitory effect of a series of aromatic thiosemicarbazone analogues on the mushroom tyrosinase activity and evaluate the kinetic parameters and the inhibition mechanisms. Based on structural information of tyrosinase, 19 thisosemicarbazones with different hydrophobic substituents were synthesized. Cytotoxicity of presented compounds against murine melanoma B16F10 cell line and their effectiveness in inhibition of melanin production has been also investigated . The molecular docking have been also performed to compare the wet lab results with theoretical calculations. These outcomes could be used to provide the basis for developing novel effective tyrosinase

inhibitors and searching for new whitening agents in cosmetic preparations or anti-browning agents for food products.

2. Results and discussion

2.1. Chemistry

The synthesis of the title compounds is shown in **Scheme 1.** All the thiosemicarbazones (TSCs) were prepared in the reaction of carbonyl compounds (ketones or aldehydes) with thiosemicarbazide or *N*(4)-substituted thiosemicarbazides. The reaction was carried out in boiling ethanol in the presence of acetic acid or *p*-toluenesulfonic acid as catalyst.

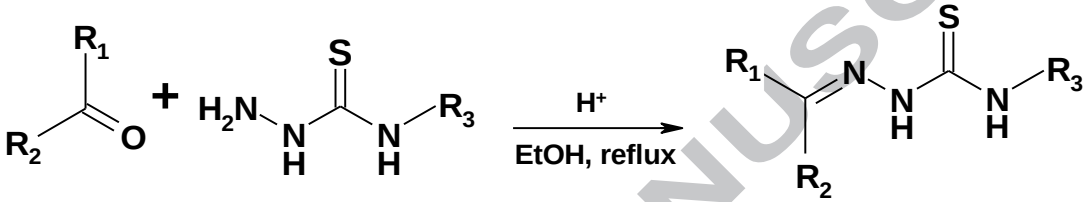

Scheme 1. General procedure for the synthesis of investigated thiosemibcarbazones

Crude TSCs were precipitated with aqueous sodium bicarbonate solution, separated by filtration and subsequently recrystallized. In the case of semisolid/oily TSCs (8-10) they were extracted with dichloromethane. In the case of *N*(4)-substituted TSCs, *N*(4)-substituted thiosemicarbazides were first prepared by the reaction of appropriate isothiocyanates with hydrazine hydrate in isopropyl alcohol. All thiosemicarbazones were characterized by ^{1}H NMR, ^{13}C NMR and HRMS.

From the all prepared TSCs only phenyl isopropyl ketone thiosemicarbazone 4 was obtained as a mixture of *E* and *Z* isomers, while other TSCs were obtained as single isomers. It is noteworthy that in many cases of thiosemicarbazones described in the literature, the problem of formation of *E* and/or *Z* isomers is completely omitted. However, it is proved that in the case of typical aromatic aldehydes and aryl alkyl ketones *E* isomer is predominantly preferred [33-36], while formation of *Z* isomer can become favorable by intramolecular hydrogen bonding [37, 38, 39, 40], especially in the case of *N*(4) disubstituted thiosemicarbazones [41]. Both isomers can be readily distinguish on the basis of ^{1}H NMR. The diagnostic signal in the analysis of the geometry of the C=N double bond of TSCs is the signal of N^{2}H proton (C=N-N*H*-) [36, 42, 43]. For *E* thiosemicarbazones derived from the aryl alkyl ketones the signal of N^{2}H proton is in the range of ~10.2-10.6 ppm [20,44,45], while in case of aromatic aldehydes derivatives the corresponding signal is usually shifted downfield to over 11 ppm [36, 44].

In the case of aldehydes-derived TSCs 1 and 19 the N^{2}H signals were observed at 11.44 and 11.66 ppm, respectively. The aryl alkyl ketone derivatives (TSCs 2-3, 5-12 and 14-18) exhibit the signals of N^{2}H protons at 10.23-10.60 ppm. Therefore, the ^{1}H NMR studies in DMSO-d_6 solution together with literature data confirm that thiosemicarbazones 1-3, 5-12 and 14-19 exist as *E* isomers. Due to the Cahn-Ingold-Prelog priority rules, the same orientation of substituents attached to the C=N carbon in the case of 2,2,2-trifluoroacetophenone thiosemicarbazone 13 translates to formally *Z* isomer.

In the case of thiosemicarbazone 4 which exhibits two sets of signals, chemical shift of the N^{2}H signal of the minor isomer (10.29 ppm) suggests *E* configuration, that might indicate

that the second N^2H signal of the major isomer (8.20 ppm) corresponds to the *Z* isomer. To verify this hypothesis, 2D NMR NOESY (Nuclear Overhauser Effect Spectroscopy) experiment was performed. There correlation between N^2H signal at 10.29 ppm and methine proton of the isopropyl group at ~3.5 ppm was observed, what confirms that the minor isomer of TSC 4 has *E* configuration. While, the NOE interaction of the N^2H signal at 8.20 ppm with the *ortho* protons of the phenyl group is a strong evidence for *Z* configuration of the major isomer. The *discrepancies* between the chemical shifts of the signals for N^2H proton in 4 assigned as *Z* isomer (8.20 ppm) and the chemical shifts of typical *Z* thiosemicarbazones (14-15 ppm) may be due to the fact that known examples are heterocyclic and the *Z* conformation is promoted by intramolecular hydrogen bond between the N^2H and heterocyclic nitrogen while in the case of 4 it seems that the steric effect of isopropyl group determines geometry. Thiosemicarbazone 4 is described in the literature as a single isomer and the given ^1H NMR data corresponds to *Z* isomer [46]. Furthermore, thiosemicarbazone 4 is also described in other papers, while without any NMR data or information on E/Z isomer ratio [45, 47].

2.2. Kinetic studies

Among different types of tyrosinase, mushroom tyrosinase has the highest homology with the mammalian tyrosinase [48]. Moreover, because of convenient assay method, the high activity and commercial availability mushroom tyrosinase has become a model system for studying tyrosinase activity and inhibition.

Buitrago *et al*. [29] reported kinetics of interaction with mushroom tyrosinase for benzaldehyde thiosemicarbazone. This compound revealed strong inhibition potency with K_i of 0,93 µM. Based on this result, we decided to test other 18 thiosemicarbazone analogues as the inhibitors of oxidation of L-dopa by tyrosinase from mushroom. Kojic acid, a well-known tyrosinase inhibitor [49,50] was used as positive control. The inhibition type and the inhibition constants (K_i and αK_i) were determined using methods as described by Copeland [51]. The results are shown in **Table 1.**

Table 1. Structures and results of kinetic studies of all target compounds.

Compound	R1	R2	R3	Inhibition type	K_I (µM)	αK_I(µM)
TSC 1		-H	-H	noncompetitive	3.7 ± 0.1	3.7 ± 0.1
TSC 2		$-CH_3$	-H	competitive	0.38 ± 0.1	-
TSC 3		-Et	-H	mixed	20.0 ± 0.2	85.5 ± 0.8
TSC 4		*i*-Pr	-H	mixed	454.6 ± 0.3	577.5 ± 0.3
TSC 5		*n*-Pr	-H	mixed	507.5 ± 0.5	>1000
TSC 6		*i*-Bu	-H		No inhibition effect	
TSC 7		*n*-Bu	-H	mixed	826.3 ± 0.2	>1000
TSC 8		*n*-pentyl	-H	uncompetitive	–	26.2 ±1.0
TSC 9		*n*-hexyl	-H	mixed	59.9 ± 0.3	330.4 ± 0.2
TSC 10		*n*-undecyl	-H		No inhibition effect	
TSC 11			-H	mixed	0.58 ± 0.07	2.6 ± 0.2
TSC 12			-H		No inhibition effect	
TSC 13		$-CF_3$	-H	mixed	293.1 ± 0.2	889.4 ± 0.4

TSC 14		$-CH_3$	$-CH_3$	competitive	202.3 ± 2.1	-
TSC 15		$-CH_3$		noncompetitive	10.9 ± 0.5	10.9 ± 0.5
TSC 16		$-CH_3$		uncompetitive	-	52.4 ± 0.2
TSC 17		$-CH_3$		mixed	432.3 ± 3.4	602.8 ± 3.7
TSC 18		$-CH_3$	-H	mixed	0.83 ± 0.16	1.4 ± 0.2
TSC 19		-H	-H	competitive	37.5 ± 0.7	-
	Kojic acid			mixed	10.2 ± 0.2	138.7 ± 1.7

2.2.1. Type of inhibition

The inhibition type was determined by the Lineweaver-Burk plot based on the results of inhibitory effect of the compounds on the diphenolase activity of tyrosinase.

TSC 3-5, 7, 9, 11, 13, 17, 18 revealed mixed pattern of inhibition what means that they have affinity to both, free enzyme and enzyme-substrate complex. In all cases of mixed-type inhibitors affinity to the free enzyme is much higher than to the enzyme-substrate complex (K_i values are lower then αK_i) so K_i value will be used for further comparison of these compound in this work.

Compounds 1 and 15 turned out to be non-competitive inhibitors (equal affinity to the free enzyme and enzyme-substrate complex). Compounds 2, 14 and 19 inhibit tyrosinase competitively, binding to its active site and compounds 8 and 16 have affinity only to the enzyme-substrate complex.

2.2.2. Inhibition constants

Inhibition constants K_i were determined by the secondary plots of apparent K_m versus the inhibitor concentration for competitive inhibition and by the secondary plots of the slope of the lines from the Lineweaver-Burk plot as a function of the inhibitor concentration for non-competitive and mixed-type inhibition. Inhibition constant αK_i was determined by the secondary plots of $1/V_{max}$ as the function of the inhibitor concentration for uncompetitive and mixed-type inhibition.

Kojic acid, well known and the most intensively studied tyrosinase inhibitor is often used as a positive standard when the new inhibitors are investigated [49, 50]. All inhibition constants of investigated compounds were compared with the one for kojic acid. Compounds 1, 2, 11 and 18 revealed better inhibitory properties than kojic acid (K_i = 10,2 µM). Compounds 2, 11 and 18 are the most potent tyrosinase inhibitors out of investigated thiosemicarbazones as their inhibition constants are lower than 1 µM. Compound 2 is 27 times stronger inhibitor than kojic acid, compound 11 18 times stronger and compound 18 is 12 times stronger.

In our investigations, benzaldehyde thiosemicarbazone (TSC 1) exhibited Ki value of 3,7 µM what is 4 times higher value than the one reported in [29] but still we can consider TSC 1 as a potent inhibitor (3 times better inhibitory activity than kojic acid).

Fig. 1. presents Lineweaver-Burk plots and secondary plots for two most potent tyrosinase inhibitors investigated in this study (TSC 2 and TSC 11).

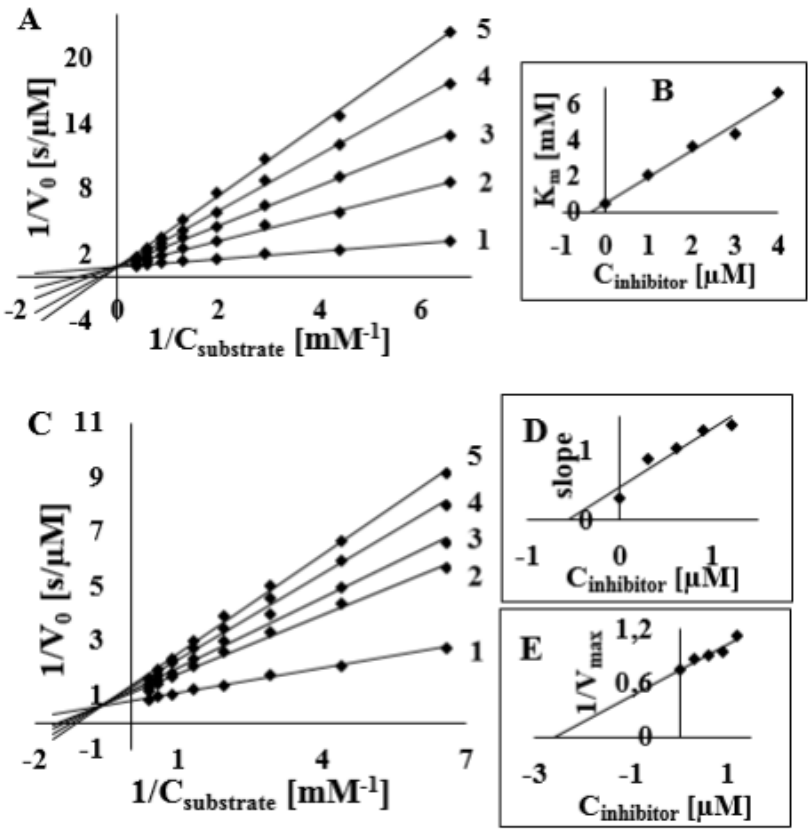

Fig. 1. Lineweaver-Burk plots for inhibition of TSC 2 (A) and TSC 11 (C) on mushroom tyrosinase with L-DOPA as substrate. The concentrations of TSC 2 for curves 1-5 are 0.0, 1.0, 2.0, 3.0 and 4.0 µM, respectively. The concentrations of TSC 11 for curves 1-5 are 0.0, 0.3, 0.6, 0.9 and 1.2, respectively. B, D and E are secondary plots of K_m, slopes (from Lineweaver-Burk plots) and $1/V_{max}$, respectively, versus inhibitor concentrations for determination of inhibitory constants.

2.2.3. Inhibition mechanism of TSC 2 and TSC 11 on the diphenolase activity of tyrosinase

Inhibition mechanism indicates if investigated compound inhibits the enzyme activity in reversible or irreversible mode.

Reversible and irreversible inhibitors can be distinguished by plotting reaction velocity versus enzyme concentration or total units of enzyme activity added to the assay. For a reversible inhibition, curves representing "plus inhibitor" have smaller slopes than the control curve and goes through the origin. For irreversible inhibition, the "plus inhibitor" curves have the same slope as the control curve (they are parallel) but intersect the 'X' axis at a position equivalent to the amount of enzyme that is irreversibly inactivated.

The inhibition mechanism of TSC 2 and TSC 11 on tyrosinase for diphenolase activity was tested using standard graphical method that is usually used for determining inhibition mechanism [13,14,25]. Both compounds revealed the same manner of inhibitory activity. As shown in **Fig. 2.** the plots representing the remaining tyrosinase activity versus the enzyme concentration at different inhibitor concentrations (with constant substrate concentration - L-DOPA) gave a family of straight lines which all passed through the origin of the coordinate system.

TSC 2 and TSC 11 are reversible inhibitors of tyrosinase. The presence of inhibitor did not bring down the amount of active enzyme but just led to a decrease in the enzyme activity (velocity).

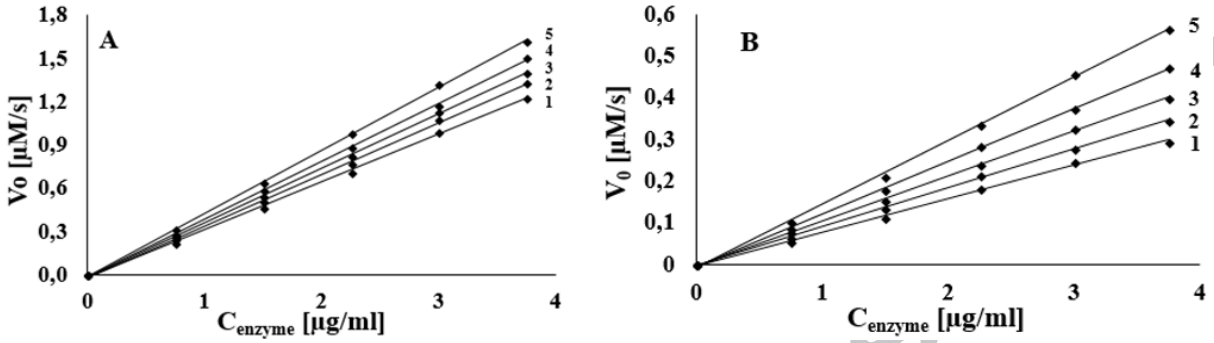

Fig. 2. The plots of inhibitory mechanism of TSC 2 (A) and TSC 11 (B) on mushroom tyrosinase with L-DOPA as substrate. The concentrations of TSC 2 for curves 1-5 are 4.0, 3.0, 2.0, 1.0 and 0.0 µM, respectively. The concentrations of TSC 11 for curves 1-5 are 1.2, 0.9, 0.6, 0.3 and 0.0, respectively.

2.2.4. Structure-activity relationship

The general structure of thiosemicarbazones examined in this work is shown in **Fig. 3.**

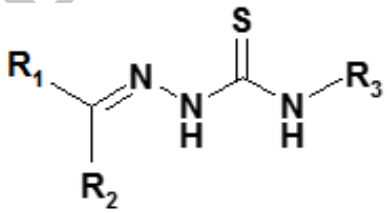

Fig. 3. The general structure of thiosemicarbazone derivatives

Effect of R_1, R_2 and R_3 substituents on the biological activity is discussed as follows.

Substitution of phenyl group with naphthyl group in position R_1 increased K_i value from 0,38 (compound 2) to 0,83 (compound 18) but still the inhibitor is considered as a very potent one. Substitution of phenyl group with bigger anthracenyl group increased K_i value 10 times what can be related with the size of anthracenyl group and lower ability of fitting to the active site of the enzyme.

There is no clear relationship between elongation of alkyl chain in position R_2 and the strength of interaction with the enzyme. Generally we can say that the shorter chain effects in the more potent inhibitor (proton, methyl and ethyl groups have K_i 3,7 and 0,38 and 20,0 µM, respectively. Elongation of alkyl chain to C-3 and C-4 increased K_i values more than 10 times and for *iso*-butyl there is no inhibition effect. What is interesting, compound 8 (with n-pentyl group) has relatively low value of inhibition constant but it can interact only with enzyme-substrate complex and compound 9 (with *n*-hexyl group) also exhibited stronger potency than TSCs with propyl and butyl substituents. Elongation of the chain to linear C-11 results in no inhibitory activity of the investigated compound. Phenyl group is almost as potent as methyl

group giving K_i of 0,58 μM but substitution of phenyl group with benzyl one led to total loss of inhibitory activity what suggests that the distance of aromatic ring in position R2 from the rest of the TSC molecule is crucial for its inhibition ability. The try of substitution of hydrophobic methyl group with more hydrophilic trifluoromethyl group increased K_i value almost 800 times.

Proton seems to be the best substituent in position R_3. Substitution with methyl group increased the K_i value about 500 times. Phenyl group in this position exhibits significant impact on inhibitory ability in comparison with methyl group but still is worse than proton. An increase the distance of aromatic ring from the thiosemicarbazide moiety decreased the inhibitory activity of these compounds.

2.3. Molecular docking

The understanding of the physical nature of ligand-receptor interaction is crucial for understanding molecular assembly of this complex and for understanding mode of inhibitory action.

Optimized conformations of the inhibitors were obtained using the Gaussian09 at the B3LYP/6-311g(d,p) level of theory [52] with the solvent model and consequently they were docked to the active site of tyrosinase, available from Protein Data Bank [53] using AutoDock software [54]. To perform accurate docking procedure in AutoDock good assignment of charges on ligand is required. Therefore they have been obtained from the *ab initio* calculations with Merz-Singh-Kollman scheme [55]. Structure of tyrosinase was protonated at pH 6.8 using H+ web server [56,57]. In the case of uncompetitive and mixed inhibitors, docking to the structure of tyrosinase has been performed with the predocked L-dopa.

As a result of docking process the clusters representing different binding manner have been obtained for each ligand. The most probable assignments of investigated ligands in the tyrosinase active site based on docking simulation are reported in **Table S1.** Multiple clusters have been specified for the thiosemicarbazones with the aromatic ring in position R1 or R2 localized in the active site in close contact to catalytic copper ions. The most important information is delivered by combining the cluster size and the binding energy between the inhibitor molecule and the enzyme active site. From the obtained results it could be concluded, that the best inhibitory properties are found for the following compounds TSC 19, TSC 2, TSC 3 and TSC 18.

The magnitude of interaction of these inhibitors in the enzyme active site is described by the highest total absolute value of the binding energy for the biggest clusters.

The docking of these molecules in the active site is shown in **Fig. 4.** According to this Figure, inhibitor-enzyme complexes shown on A, C, D, E, G, H, I and J diagrams are stabilized by at least two intermolecular hydrogen bonds. Moreover, in the case of TSC 2, strong π-π interaction between phenyl ring of inhibitor and side chain of His263 stabilizes the inhibitor arrangement in the enzymatic active pocket (see **Fig. 4. D**). Only cluster 2 found for TSC 11 presents orientation of the inhibitor which could allow to complex the copper ions by the thiourea moiety (see **Fig. 4. J**) what was reported for such compounds by Xie *et al*. [24] and Buitrago *et al*. [29]. Based on manual docking and following molecular dynamic simulation, Buitrago *et al.*, suggest that TSC 1 is able to decrease the enzyme activity due to interaction between thiosemicarbazide moiety of inhibitor and catalytic copper ions of tyrosinase [29]. Results of simulation of docking process in current work reveal a different way of interaction with the enzyme active site. Achieved results show that TSC 1 is able to inhibit tyrosinase, indeed. However, the found alignment of the inhibitor is similar to the one of the enzyme's substrate (cluster 2 – see **Fig. 4. B**). This scheme of interaction is not the most probable and most favorable one, though. This example is represented by cluster 1 (see

Fig. 4. B) which includes almost 50% of all docked structures and is characterized by the mean binding energy lower than for cluster 2 of about 0.2 kcal/mol.

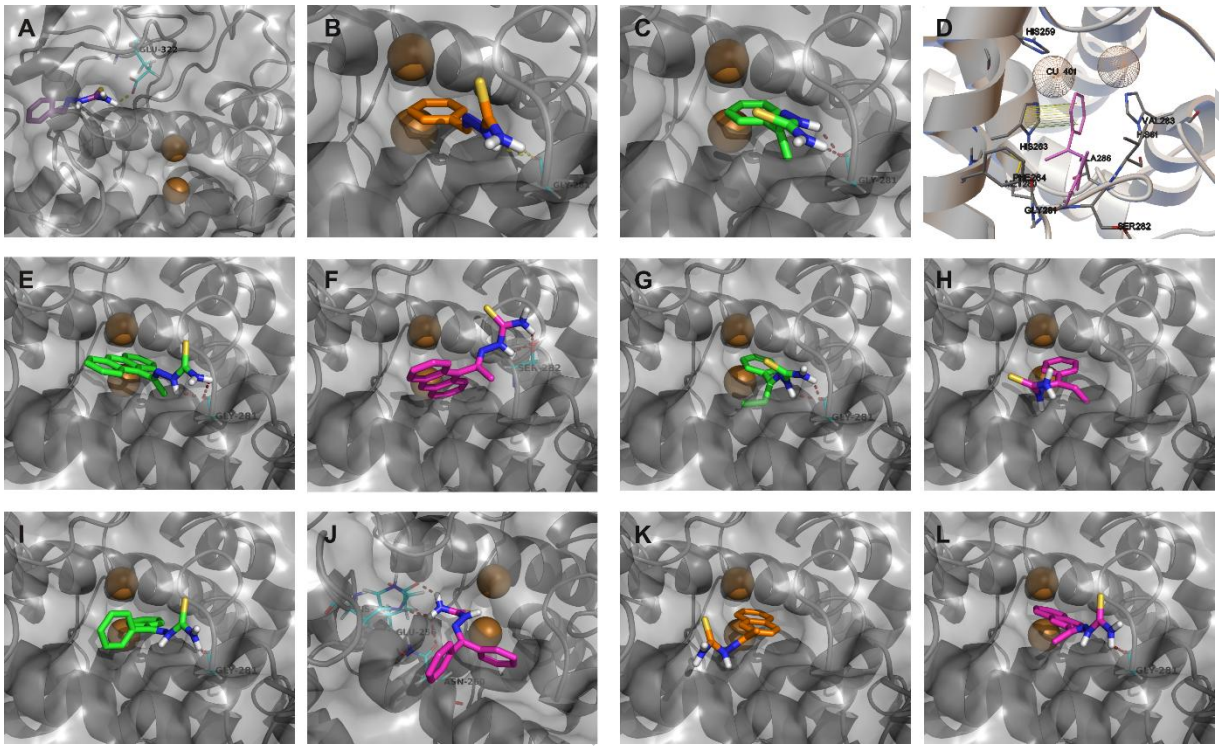

Fig. 4. Orientation of the selected inhibitors in the active site of tyrosinase (copper ions are represented by *orange spheres* and interatomic hydrogen bonds by *dashed lines*); A) TSC 1 cluster 1; B) TSC 1 cluster 2; C) TSC 2; D) TSC 2 with marked π-π interactions; E) TSC 19 cluster 1; F) TSC 19 cluster 2; G) TSC 3 cluster 1; H) TSC 3 cluster 2; I) TSC 11 cluster 1; J) TSC 11 cluster 2; K) TSC 18 cluster 1; L) TSC 18 cluster 2.

2.4. Effectiveness of TSCs in melanogenesis inhibition

For the purpose of screening of antimelanogenic effects, B16F10 melanoma cells are widely used, because they are relatively easy to culture *in vitro*, and they share most of the melanogenic mechanisms of normal human melanocytes [58].

In order to test the inhibitory effect of the studied TSCs on melanogenesis, B16 mouse melanoma cells were stimulated with α-MSH, which is physiological stimulator of the pigmentation. During 48 hours of hormonal stimulation, cells were treated with the inhibitors at various concentration (1-100 μM). Kojic acid was used as a positive control. B16 cell viability was also estimated in the presence of the tested inhibitors.

Fig. 6. represents percentage inhibition of melanin production in B16 cells. TSC 2, 3, 6, 8, 9, 10, 13 and 18 fully inhibit this process even at the inhibitor concentration of 10 μM. Only TSC 1, 14 and 17 exhibit value of inhibition lower than 50%. All investigated thiosemicarbazones reveal stronger inhibition in comparison with kojic acid.

Melanin production in B16 cells was inhibited by TSC 1-19 in dose-dependent manner. **Table 2.** shows IC_{50} values of this process for comparison to results presented in the **Fig. 5.** All of investigated compounds showed strong potency of melanogenesis inhibition (low IC_{50} values in comparison with positive control – kojic acid). Compounds with IC_{50} value between 1 and 5 μM (TSC 2, 4, 7, 11, 12, 13, 16, 18 and 19) were classified as strong inhibitors and exhibited more than 5 times stronger inhibition ability than kojic acid. In turn, compounds

with IC_{50} value less than 1 µM (TSC 3,5,6, 8-10) could be considered as very strong melanogenesis inhibitors (more than 30 times stronger inhibition potency than kojic acid).

These results were verified with the effect of tested inhibitors on proliferation of B16 cells (see **Table 2**.). The decrease in melanin production might be caused by high toxicity of the inhibitors which, in turn, can lead to the inhibition of cell proliferation.

Cells treated with inhibitors: 10, 15, 18 and 19 produced low amount of melanin. However, these results might be caused by high toxicity of the inhibitors (IC_{50}<10 µM) which led to the inhibition of cell proliferation. Inhibitors which revealed strong melanogenesis inhibitory effect and did not cause high inhibition of proliferation may be considered as potent, non-toxic inhibitors of melanin biosynthesis pathway in B16 cells (TSC 2, 3, 4, 5, 6, 7, 8, 9, 11, 12, 13, 16).

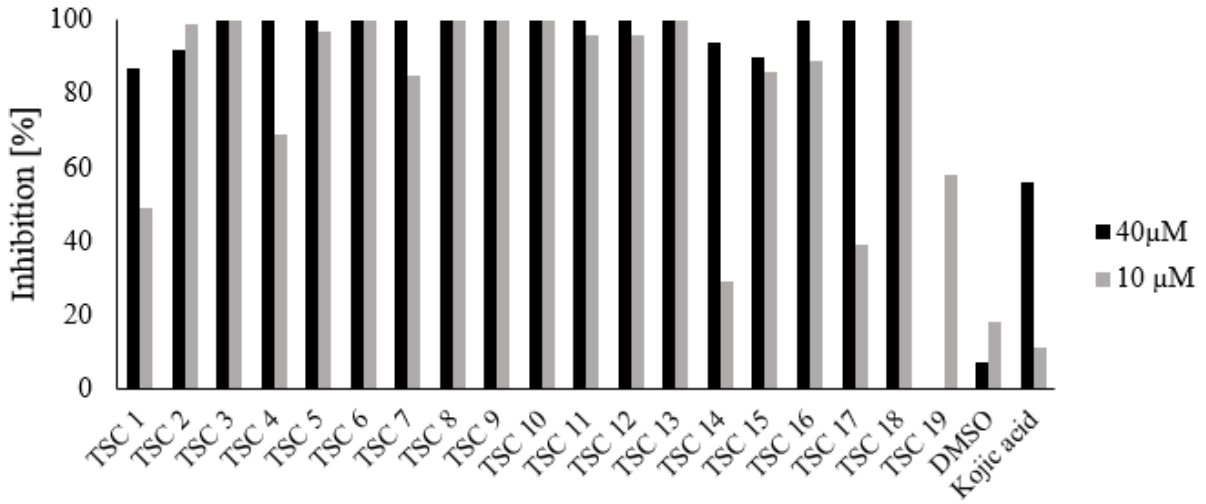

Fig. 5. Percentage inhibition of melanin production in B16 cells at inhibitor concentrations of 40 and 10 µM. Kojic acid was positive control, whereas DMSO was control of TSC solvent. With respect to the TSC 19 the proper absorbance measurement at 40 µM was unachievable because of the compound color.

Table 2. Inhibition of melanin production and cell proliferation in B16 cells.

Compound	Inhibition of melanin production IC_{50} (µM)	95% CI IC_{50}	Inhibition of cell proliferation IC_{50} (µM)	95% CI IC_{50}
TSC 1	10.2	9.1 - 11.4	54.6	45.9 - 64.8
TSC 2	2.0	1.4 - 2.9	19.6	13.7 - 28.1
TSC 3	<1.0	0.7 - 1.9	32.3	19.2 - 54.3
TSC 4	2.3	1.4 - 3.6	28.5	22.3 - 36.5
TSC 5	<1.0	0.05 - 9.1	25.5	18.6 - 35.1
TSC 6	<1.0	0.01 - 5.6	27.3	19.1 - 39.2
TSC 7	1.2	0.7 - 1.8	36.8	27.4 - 49.5
TSC 8	<1.0	0.2 - 1.4	34.6	24.4 - 49.1
TSC 9	<1.0	NA	10.8	7.0 - 16.8
TSC 10	<1.0	NA	2.5	1.6 - 4.0
TSC 11	1.4	1.0 - 1.8	43.6	33.7 - 56.4

TSC 12	1.3	0.7 - 2.4	49.5	41.2 - 59.5
TSC 13	4.7	3.2 - 6.8	131.8	97.3 - 178.7
TSC 14	14.8	12.0 - 18.4	62.4	37.0 - 105.3
TSC 15	5.2	4.7 - 5.9	7.5	5.4 - 10.2
TSC 16	4.7	4.4 - 5.1	14.4	11.5 - 18.2
TSC 17	11.6	9.5 -14.2	21.1	18.2 - 24.4
TSC 18	1.8	1.5 - 2.3	2.7	1.9 - 3.9
TSC 19	1.0	0.3 - 3.8	5.7	4.1 - 7.9
DMSO	98.9	63.8 – 153.2	252.5	235.1 – 271.1
Kojic acid	32.2	26.3 – 39.5	181.3	150.6 – 218.3

3. Conclusions

In the frame of this work, 19 thiosemicarbazones were synthesized and its inhibitory activity toward mushroom tyrosinase was examined. Moreover, molecular docking of these compounds to the active site of the enzyme was performed and ability to inhibition of melanogenesis in B16 cells was checked.

Kinetic studies of inhibition of diphenolase activity of tyrosinase revealed that there is a correlation between structure of investigated molecules and its inhibitory activity. The influence of substituents in R_1, R_2 and R_3 positions on thiosemicarbazone inhibitory abilities was investigated. Phenyl ring in R_1 enables the best inhibition of enzyme in comparison with naphthyl and anthracenyl substituents. In R_2, methyl and phenyl groups are favorable. Elongation and branching of alkyl chain diminishes the inhibitory potential of TSCs. With respect to R_3, the replacement of proton decreases the activity of inhibitors. Abovementioned observations indicate that the smaller and less branched molecules exhibit higher affinity to enzyme what might be associated with the steric constraints. The fact that TSCs demonstrate different types of inhibition (competitive, noncompetitive, uncompetitive and mixed type) proves their affinity to both: free enzyme and substrate-enzyme complex.

Molecular docking studies show that in the majority of the cases TSCs interact rather with tyrosinase active site via aromatic ring than thiosemicarbazide moiety what can be helpful information in designing novel tyrosinase inhibitors.

Most of investigated compounds reveals very good inhibitory activity against melanin production in B16 cells. There is no obvious relationship between inhibition of melanogenesis in melanoma cells and enzyme inhibition. Moreover, in the case of melanogenesis, elongation of alkyl chain in R_2 position seems to have a positive impact on inhibition. It can be predicted then that most of melanogenesis inhibitors described above inhibit the pathway also on the other stages than the step catalyzed by tyrosinase, for example affecting activity of other key enzymes in melanin biosynthesis like dopachrome tautomerase, microphthalmia associated transcription factor or tyrosinase related protein 1 [59].

Results of our studies show that thiosemicarbazones can be considered as potent inhibitors of tyrosinase and melanogenesis.

4. Experimental

4.1. Chemistry

General information: The ^{1}H and ^{13}C NMR spectra were recorded on a 600 MHz Bruker Avance and Jeol ECZ 400S spectrometers in DMSO - d_6 as solvent. Chemical shifts (δ) are given in parts per million (ppm) relative to solvent signals (2.50 ppm and 39.52 ppm in ^{1}H NMR and in ^{13}C NMR spectra, respectively). Multiplicity is reported as follows: s = singlet, d = doublet, t = triplet, q = quartet, quint = quintet, sext = sextet, hept = heptet, m = multiplet, br = broad. High-resolution Mass Spectra were recorded on an LCT Premier XE Waters apparatus, on ESI+ mode. All solvents were of commercial quality and purchased from a local supplier. Starting carbonyl compound, thiosemicarbazide, methyl isothiocyanate, phenyl isothiocyanate, phenethyl isothiosyanate and other reagents were purchased from Sigma-Aldrich. Benzyl isothiocyanate was prepared by literature procedure [60]. No procedures or isolations of products were optimized.

4.1.1. General Procedure for preparation of N^4-substituted thiosemicarbazide

Hydrazine monohydrate (0.12 mol, ~6 mL) was added dropwise to a stirred solution of the appropriate isothiocyanate (0.10 mol) in 2-propanol (75 mL) in 15-20 minutes at 0 °C (water-ice bath). The resulting suspension was left for ~ 30 minutes at 0 °C and ~1 hour at room temperature. Then the product was filtered, washed with 2-propanol (4 × 25 mL) and diethyl ether (2 × 50 mL) and dried on air. Obtained crude N^4-substituted thiosemicarbazides were sufficiently pure (based on ^{1}H NMR) and used in the next step without further purification.

4.1.1.1. 4-Methylthiosemicarbazide

Yield 85%; ^{1}H NMR (600MHz, DMSO-d_6) δ: 2.90 (s, 3H, C*H*$_3$), 4.42 (bs, 2H, N*H*$_2$), 7.81 (bs, 1H, N*H*), 8.56 (s, 1H, N*H*).

4.1.1.2. 4-Phenylthiosemicarbazide

Yield 91%; ^{1}H NMR (600MHz, DMSO-d_6) δ: 4.76 (bs, 2H, N*H*$_2$), 7.11 (t, 1H, *J*=7.3 Hz, Ar*H*), 7.31 (t, 2H, *J*=8.1 Hz, Ar*H*), 7.64 (bd, 2H, *J* not resolved, Ar*H*), 9.07 (s, 1H, N*H*), 9.65 (bs, 1H, N*H*). NMR spectrum is in agreement with data reported in literature [61].

4.1.1.3. 4-Benzylthiosemicarbazide

Yield 61%; ^{1}H NMR (600MHz, DMSO-d_6) δ: 4.52 (bs, 2H, N*H*$_2$), 4.72 (d, 1H, *J*=6.2 Hz, C*H2*), 7.22-7.25 (m, 1H, Ar*H*), 7.29-7.33 (m, 4H, Ar*H*), 8.38 (bs, 1H, N*H*), 8.75 (s, 1H, N*H*). NMR spectrum is in agreement with data reported in literature [62]

4.1.1.4. 4-Phenethylthiosemicarbazide

Yield 86%; ^{1}H NMR (600MHz, DMSO-d_6) δ: 2.83 (t, 2H, *J*=7.5 Hz, C*H2*), 3.68 (dt, 2H, *J*=6.6 Hz, *J*=7.6 Hz, NC*H2*), 4.44 (s, 2H, N*H*$_2$), 4.72 (d, 1H, *J*=6.2 Hz, C*H2*), 7.21 (t, 1H, *J*=7.2 Hz, Ar*H*), 7.25 (d, 2H, *J*=7.4 Hz, Ar*H*), 7.31 (t, 2H, *J*=7.4 Hz, Ar*H*), 7.88 (bs, 1H, N*H*), 8.65 (s, 1H, N*H*). NMR spectrum is in agreement with data reported in literature [63].

4.1.2. General Procedure for preparation of thiosemicarbazones 1-19 (**TSCs 1-19**).

The mixture of carbonyl compound (0.020 mol) and thiosemicarbazide (1.9 g, 0.021 mol for TSCs 1-8 and 18-19 or 5.5 g, 0.060 mol for TSCs 9-13) or the appropriate N^4-substituted thiosemicarbazide (0.021 mol for 14-17) and acid catalyst (~2 mL of acetic acid for 1-8, 19 or *p*-toluenesulfonic acid monohydrate, 3.8g, 0.02 mol for 9-18) in 96% ethanol (50 mL) was refluxed for about 8 hours. After cooling to room temperature, the mixture was added in few portions to vigorously stirred 10% sodium bicarbonate solution (150 mL) and stirring was

continued for about 30 min. The resulting solid was filtered, washed with water (2 × 50 mL, 10 × 20 mL) and dried on air giving a crude TSC. Analytical samples were obtained by crystallization from appropriate solvent: 96% EtOH for 1- 3, 7, 11-17 and 19; 75% aq. EtOH for 4 and 6; anh. EtOH: petroleum ether (2:3, V/V) for 5; MeOH for 18. In case of 8-10, the suspension in aq. $NaHCO_3$, was extracted with dichloromethane (1 × 50 mL, 2 × 25 mL). The combined organic phase was washed with water (5 × 30mL), dried over anh. Na_2SO_4, and concentrated under reduced pressure, to give the products 8-10 as thick oils, which partially solidified after standing at room temperature. These TSC were used without further purification.

4.1.2.1. (E)-Benzaldehyde thiosemicarbazone (**TSC 1**).

Yield 31 %; ^{1}H NMR (600MHz, DMSO-d_6) δ: 7.38-7.43 (m, 3H, Ar*H*), 7.79-7.81 (m, 2H, Ar*H*), 8.00 (s, 1H, N*H*), 8.06 (s, 1H, C*H*=N), 8.21 (s, 1H, N*H*), 11.44 (s, 1H, N*H*). ^{13}C NMR (100 MHz, DMSO-d_6) δ: 127.82, 129.18,134.70, 134.70, 142.79 (*C*=N), 178.51 (*C*=S). HRMS (ESI+): *m*/*z* calcd for $C_8H_{10}N_3S$ $(M+H)^+$ 180.0595, found 180.0592. NMR spectra are in agreement with data reported in literature [64,65].

4.1.2.2. (E)-Acetophenone thiosemicarbazone (**TSC 2**).

Yield 69%; ^{1}H NMR (600MHz, DMSO-d_6) δ: 2.31 (s, 3H, C*H*$_3$), 7.38-7.40 (m, 3H, Ar*H*), 7.92-7.94 (m, 3H, N*H* + Ar*H*), 8.29 (bs, 1H, N*H*), 10.23 (s, 1H, N*H*). ^{13}C NMR (100 MHz, DMSO-d_6) δ: 14.54 (*C*H$_3$), 127.11, 128.76, 129.73, 138.16, 148.38 (*C*=N), 179.45 (*C*=S). HRMS (ESI+): *m*/*z* calcd for $C_9H_{12}N_3S$ $(M+H)^+$ 194.0752, found 194.0782. NMR spectra are in agreement with data reported in literature [44,66].

4.1.2.3. (E)-Propiophenone thiosemicarbazone (**TSC 3**).

Yield 78%; ^{1}H NMR (600MHz, DMSO-d_6) δ: 1.03 (t, 3H, *J*=7.8 Hz, C*H*$_3$), 2.88 (q, 2H, *J*=7.8 Hz, C*H*$_2$), 7.39-7.41 (m, 3H, Ar*H*), 7.90-7.93 (m, 3H, N*H* + *ArH*), 8.29 (bs, 1H, *NH*), 10.35 (s, 1H, *NH*). ^{13}C NMR (100 MHz, DMSO-d_6) δ: 11.50 (*C*H$_3$), 19.77, 127.21, 128.90, 129.68, 136.92, 152.30 (*C*=N), 179.49 (*C*=S). HRMS (ESI+): *m*/*z* calcd for $C_{10}H_{14}N_3S$ $(M+H)^+$ 208.0909, found 208.0949. ^{1}H NMR spectrum is in agreement with data reported in literature [46,67].

4.1.2.4. Mixture of Z and E isomers (in 89:11 molar ratio) of isobutyrophenone thiosemicarbazone (**TSC 4**).

Yield 82%; ^{1}H NMR (600MHz, DMSO-d_6) δ: 1.08 (d, *J*=6.8 Hz, C*H*$_3$, *Z* isomer) and 1.12 (d, *J*=7.0 Hz, C*H*$_3$, *E* isomer) [total integration 6H], 2.83 (hept, *J*=6.8 Hz, C*H*, *Z* isomer) and 3.56 (hept, *J*=7.0 Hz, C*H*, *E* isomer) [total integration 1H], 7.27 (d, *J*=8.1 Hz, Ar*H*, *Z* isomer) and 7.38 (m, Ar*H*, *E* isomer) [total integration 2H], 7.52 (m, Ar*H*, *E* + *Z* isomers) and 7.58 (t, Ar*H*, *J*=7.3 Hz, *Z* isomer) [total integration 3H], 7.66 (bs, *NH*, *E* isomer) and 7.79 (bs, *NH*, *Z* isomer) [total integration 1H], 8.24 (bs, 1H, N*H*, *E* + *Z* isomers). 8.45 (s, 1H, NH, *Z* isomer) and 10.33 (s, 1H, NH, *E* isomer) [total integration 1H]. ^{13}C NMR (100 MHz, DMSO-d_6) δ: major, *Z* isomer: 20.39, 36.04, 127.70, 129.99, 158.38, 178.37*; minor *E* isomer: 20.28, 27.64, 128.46, 128.51, 128.87, 137.57, 157.48, 179.64; * one aromatic *C*H carbon signal is missing, probably due to coalescence and overlaps. HRMS (ESI+): *m*/*z* calcd for $C_{11}H_{15}N_3S$ $(M+H)^+$ 222.1065, found 222.1066. Note: the crude and recrystallized samples shown practically the same ratio of *E* and *Z* isomers.

4.1.2.5. (E)-Butyrophenone thiosemicarbazone (**TSC 5**).

Yield 73%; ^{1}H NMR (600MHz, DMSO-d_6) δ: 0.95 (t, 3H, *J*=7.5 Hz, C*H*$_3$), 1.43 (sextet, 2H, *J*=7.5 Hz, CH$_3$C*H*$_2$), 2.86 (t, 2H, *J*=7.5 Hz, C*H*$_2$), 7.39 (m, 3H, Ar*H*), 7.91 (m, 3H, NH +

ArH), 8.28 (bs, 1H,*NH*), 10.41 (s, 1H, *NH*). ^{13}C NMR (100 MHz, DMSO-d_6) δ: 14.23, 20.12, 28.11, 127.24, 128.86, 129.62, 137.35, 151.14 (*C*=N), 179.45 (*C*=S). HRMS (ESI+): *m/z* calcd for $C_{11}H_{16}N_3S$ $(M+H)^+$ 222.1065, found 222.1059.

4.1.2.6. (E)-Isovalerophenone thiosemicarbazone (**TSC 6**).

Yield 81%; ^{1}H NMR (400MHz, DMSO-d_6) δ: 0.82 (d, 6H, *J*=6.7 Hz, $(CH_3)_2CH$), 1.78 (hept, 1H, *J*=6.7 Hz, C*H*), 2.80 (d, 2H, *J*=7.3 Hz, CH_2), 7.33 (m, 3H, Ar*H*), 7.84-7.86 (m, 3H, N*H* + Ar*H*), 8.23 (bs, 1H, *NH*), 10.30 (s, 1H, *NH*). ^{13}C NMR (100 MHz, DMSO-d_6) δ: 22.42, 26.98, 34.29, 127.44, 128.79, 129.54, 137.84, 150.93 (*C*=N), 179.34 (*C*=S). HRMS (ESI+): *m/z* calcd for $C_{12}H_{18}N_3S$ $(M+H)^+$ 236.1221, found 236.1225.

4.1.2.7. (E)-Valerophenone thiosemicarbazone (**TSC 7**).

Yield 87%; ^{1}H NMR (600MHz, DMSO-d_6) δ: 0.88 (t, 3H, *J*=7.6 Hz, CH_3), 1.38 (m, 4H, $CH_3(CH_2)_2$), 2.88 (t, 2H, *J*=7.5 Hz, CH_2), 7.39 (m, 3H, Ar*H*), 7.89-7.91 (m, 3H, N*H* + Ar*H*), 8.28 (bs, 1H, *NH*), 10.38 (s, 1H, *NH*). ^{13}C NMR (100 MHz, DMSO-d_6) δ: 14.34 (CH_3), 22.57, 26.22, 28.86, 127.22. 128.86, 129.62, 137.34, 151.37 (*C*=N), 179.45 (*C*=S). HRMS (ESI+): *m/z* calcd for $C_{12}H_{18}N_3S$ $(M+H)^+$ 236.1221, found 236.1226. ^{1}H NMR spectrum is in agreement with data reported in literature [46].

4.1.2.8. (E)-Hexanophenone thiosemicarbazone (**TSC 8**).

Yield 80%; ^{1}H NMR (400MHz, DMSO-d_6) δ: 0.80 (t, 3H, *J*=7.0 Hz, CH_3), 1.20-1.37 (m, 6H, $CH_3(CH_2)_3$), 2.82 (t, 2H, *J*=7.8 Hz, CH_2), 7.32-7.35 (m, 3H, Ar*H*), 7.82-7.86 (m, 3H, N*H* + *ArH*), 8.24 (bs, 1H, *NH*), 10.34 (s, 1H, *NH*). ^{13}C NMR (100 MHz, DMSO-d_6) δ: 14.43, 22.51, 26.34, 26.39, 31.54, 127.22, 128.86, 129.62, 137.33, 151.38 (*C*=N), 179.44 (*C*=S). HRMS (ESI+): *m/z* calcd for $C_{13}H_{20}N_3S$ $(M+H)^+$ 250.1378, found 250.1390.

4.1.2.9. (E)-Heptanophenone thiosemicarbazone (**TSC 9**).

Yield 96%;^{1}H NMR (400MHz, DMSO-d_6) δ: 0.80 (t, 3H, *J*=7.0 Hz, CH_3), 1.19-1.25 (m, 4H, $CH_3(CH_2)_2$),1.25-1.40 (m, 4H, $CH_3(CH_2)_2(CH_2)_2$), 2.82 (t, 2H, *J*=7.0 Hz, CH_2), 7.30-7.35 (m, 3H, Ar*H*), 7.80-7.88 (m, 3H, NH + Ar*H*), 8.23 (bs, 1H, N*H*), 10.34 (s, 1H, N*H*). ^{13}C NMR (100 MHz, DMSO-d_6) δ: 14.45, 22.60, 26.40, 26.67, 29.00, 31.59, 127.22, 128.86, 129.60, 137.33, 151.33 (*C*=N), 179.42 (*C*=S). HRMS (ESI+): *m/z* calcd for $C_{14}H_{22}N_3S$ $(M+H)^+$ 264.1534, found 264.1540.

4.1.2.10. (E)-Dodecanophenone thiosemicarbazone (**TSC 10**).

Yield 96%; ^{1}H NMR (400MHz, DMSO-d_6) δ: 0.79 (t, 3H, *J*=7.0 Hz, CH_3), 1.10-1.25 (m, 14H, $CH_3(CH_2)_7$),1.25-1.39 (m, 4H, $CH_3(CH_2)_7(CH_2)_2$), 2.81 (t, 2H, *J*=6.7 Hz, CH_2), 7.30-7.35 (m, 3H, Ar*H*), 7.80-7.87 (m, 3H, N*H* + Ar*H*), 8.24 (bs, 1H, *NH*), 10.34 (s, 1H, *NH*). ^{13}C NMR (100 MHz, DMSO-d_6) δ: 14.47, 22.65, 26.42, 26.68, 29.28, 29.36, 29.41, 29.55, 29.56, 29.57, 31.85, 127.17, 128.81, 129.55, 137.35, 151.23 (*C*=N), 179.47 (*C*=S). HRMS (ESI+): *m/z* calcd for $C_{19}H_{32}N_3S$ $(M+H)^+$ 334.2317, found 334.2324.

4.1.2.11. Benzophenone thiosemicarbazone (**TSC 11**).

Yield 94%; ^{1}H NMR (600MHz, DMSO-d_6) δ: 7.33-7.40 (m, 4H, Ar*H*), 7.41-7.44 (m, 1H, Ar*H*), 7.61-7.65 (m, 1H, Ar*H*), 7.65-7.70 (m, 4H, Ar*H*), 8.38 (bs, 1H, *NH*), 8.41 (bs, 1H, *NH*), 8.65 (bs, 1H, *NH*). ^{13}C NMR (100 MHz, DMSO-d_6) δ: 128.11, 128.83, 128.89, 130,30, 130,38, 130,52, 131.74, 136.83, 149.61 (*C*=N), 178.37 (*C*=S). HRMS (ESI+): *m/z* calcd for $C_{14}H_{14}N_3S$ $(M+H)^+$ 256.0909, found 256.0913. NMR spectra are in agreement with data reported in literature [44,68].

4.1.2.12. (E)-2-Phenylacetophenone thiosemicarbazone (**TSC 12**).

Yield 96%; ^{1}H NMR (600MHz, DMSO-d_6) δ: 4.39 (s, 2H, CH_2), 7.14 (d, 2H, *J* = 7.8 Hz, Ar*H*), 7.19 (t, 1H, *J* = 7.3 Hz, Ar*H*), 7.29 (t, 2H, *J* = 7.8 Hz, Ar*H*), 7.36 (m, 3H, Ar*H*), 7.96 (m, 2H, Ar*H*), 8.07 (bs, 1H, N*H*), 8.40 (bs, 1H, N*H*), 10.52 (bs, 1H, N*H*). ^{13}C NMR (100 MHz, DMSO-d_6) δ: 32.24 (*C*H_2), 126.87, 127.56, 128.61, 128.83, 129.21, 129.70, 136.92, 137.42, 148.45 (*C*=N), 179.63 (*C*=S). HRMS (ESI+): *m*/*z* calcd for $C_{15}H_{16}N_3S$ $(M+H)^+$ 270.1065, found 270.1064. NMR spectra are in agreement with data reported in literature [20].

4.1.2.13. (Z)-2,2,2-Trifluoroacetophenone thiosemicarbazone (**TSC 13**).

Yield 98%;^{1}H NMR (600MHz, DMSO-d_6) δ: 7.46 (m, 2H, Ar*H*), 7.61 (m, 3H, Ar*H*), 8.10 (bs, 1H, N*H*), 8.78 (bs, 1H, N*H*), 9.87 (s, 1H, N*H*). ^{13}C NMR (150 MHz, DMSO-d_6) δ: 121.14 (q, $^{1}J_{C\text{-}F}$ = 272.8 Hz, *C*F_3), 126.74, 129.04, 130.08, 131.54, 136.20 (q, $^{2}J_{C\text{-}F}$ = 33.8 Hz C=N), 180.21 (*C*=S). HRMS (ESI+): *m*/*z* calcd for $C_9H_9F_3N_3S$ $(M+H)^+$ 248.0469, found 248.0474.

4.1.2.14. (E)-Acetophenone N(4)-methylthiosemicarbazone (**TSC 14**).

Yield 77%; ^{1}H NMR (600MHz, DMSO-d_6) δ: 2.31 (s, 3H, CH_3), 3.06 (s, 3H, NCH_3), 7.40 (m, 3H, Ar*H*), 7.93-7.95 (m, 2H, Ar*H*), 8.46 (bs, 1H, N*H*), 10.23 (s, 1H, N*H*). ^{13}C NMR (100 MHz, DMSO-d_6) δ: 14.54(*C*H_3), 31.65(N*C*H_3), 127.09, 128.75, 129.67 138.23, 148.04 (*C*=N), 179.23 (*C*=S). HRMS (ESI+): *m*/*z* calcd for $C_{10}H_{14}N_3S$ $(M+H)^+$ 208.0909, found 208.0932. ^{1}H NMR spectrum is in agreement with data reported in literature [21].

4.1.2.15. (E)-Acetophenone N(4)-phenylthiosemicarbazone (**TSC 15**).

Yield 42%; ^{1}H NMR (600MHz, DMSO-d_6) δ: 2.40 (s, 3H, CH_3), 7.22 (tt, 1H, *J* = 7.4 Hz, *J* = 1.4 Hz, Ar*H*), 7.38 (m, 2H, Ar*H*), 7.42-7.44 (m, 3H, Ar*H*), 7.58 (m, 2H, Ar*H*), 8.00-8.03 (m, 2H, Ar*H*), 10.05 (bs, 1H, N*H*), 10.60 (s, 1H, N*H*). ^{13}C NMR (100 MHz, DMSO-d_6) δ: 14.97 (*C*H_3), 125.88, 126.36, 127.39, 128.61, 128.79, 129.95, 138.02, 139.70, 149.50 (*C*=N), 177.56 (*C*=S). HRMS (ESI+): *m*/*z* calcd for $C_{15}H_{16}N_3S$ $(M+H)^+$ 270.1065, found 270.1069. ^{1}H NMR spectrum is in agreement with data reported in literature [21]

4.1.2.16. (E)-Acetophenone N(4)-benzylthiosemicarbazone (**TSC 16**).

Yield 79%; ^{1}H NMR (600MHz, DMSO-d_6) δ: 2.33 (s, 3H, CH_3), 4.88 (d, 2H, *J*= 6.4 Hz, CH_2), 7.24 (tt, 1H, *J* = 7.0 Hz, *J* = 1.9 Hz, Ar*H*), 7.31-7.36 (m, 4H, Ar*H*), 7.39-7.41 (m, 3H, Ar*H*), 7.92-7.95 (m, 2H, Ar*H*), 9.02 (bt, *J*= 6.4 Hz, 1H, N*H*), 10.31 (s, 1H, N*H*). ^{13}C NMR (100 MHz, DMSO-d_6) δ: 14.70(*C*H_3), 47.30 (*C*H_2), 127.17, 127.21, 127.70, 128.69, 128.78, 129.77, 138.18, 140.00,148.64 (*C*=N), 179.14 (*C*=S). HRMS (ESI+): *m*/*z* calcd for $C_{16}H_{18}N_3S$ $(M+H)^+$ 284.1221, found 284.1219**.**

4.1.2.17. (E)-Acetophenone N(4)-phenethylthiosemicarbazone (**TSC 17**).

Yield 86%; ^{1}H NMR (600MHz, DMSO-d_6) δ: 2.31 (s, 3H, CH_3), 2.94 (bt, 2H, *J*= 7.7 Hz, PhCH_2), 3.81 (m, 2H, NCH_2), 7.25 (tt, 1H, *J* = 7.0 Hz, *J* = 1.5 Hz, Ar*H*), 7.29-7.35 (m, 4H, Ar*H*), 7.41-7.43 (m, 3H, Ar*H*), 7.83-7.86 (m, 2H, Ar*H*), 8.46 (bt, *J*= 5.8 Hz, 1H, N*H*), 10.31 (s, 1H, N*H*). ^{13}C NMR (100 MHz, DMSO-d_6) δ: 14.64 (*C*H_3), 35.36 (*C*H_2), 45.62 (*C*H_2), 126.76, 127.02, 128.80, 129.03, 129.17, 129.76, 139.77, 140.00,148.26 (*C*=N), 178.43 (*C*=S). HRMS (ESI+): *m*/*z* calcd for $C_{17}H_{20}N_3S$ $(M+H)^+$ 298.1378, found 298.1378.

4.1.2.18. (E)-2-Acetonaphthone thiosemicarbazone (**TSC 18**).

Yield 84%; ^{1}H NMR (600MHz, DMSO-d_6) δ: 2.44 (s, 3H, CH_3), 7.54 (m, 2H, Ar*H*), 7.88 (d, 1H, *J*=8.9Hz, Ar*H*), 7.93 (m, 1H, Ar*H*), 7.99 (m, 1H, Ar*H*), 8.07 (bs, 1H, N*H*), 8.31 (dd, 1H,

J=8.9Hz, *J*=1.6Hz, Ar*H*), 8.35 (d, 1H, *J*=1.6Hz, Ar*H*), 8.36 (bs, 1H, N*H*), 10.30 (s, 1H, N*H*). ^{13}C NMR (100 MHz, DMSO-d_6) δ: 14.34 (*C*H_3), 124.63, 126.87, 127.03, 127.30, 127.96, 128.06, 129.05, 133.28, 133.76, 135.62, 148.13 (*C*=N), 179.46 (*C*=S). HRMS (ESI+): *m*/*z* calcd for $C_{13}H_{14}N_3S$ $(M+H)^+$ 244.0909, found 244.0897. NMR spectra are in agreement with data reported in literature [44,46].

4.1.2.19. (E)-9-Anthrylcarboxyaldehyde thiosemicarbazone (**TSC 19**).
Yield 75% ^{1}H NMR (600MHz, DMSO-d_6) δ: 7.59 (m, 2H, Ar*H*), 7.65 (m, 2H, Ar*H*), 7.73 (bs, 1H, N*H*), 8.16 (d, 2H, *J*=8.8Hz, Ar*H*), 8.34 (bs, 1H, *NH*), 8.58 (d, 2H, *J*=8.8Hz, Ar*H*), 8.72 (s, 1H, C*H*=N), 9.34 (s, 1H, Ar*H*), 11.66 (s, 1H, *NH*). ^{13}C NMR (100 MHz, DMSO-d_6) δ: 125.31, 125.51, 126.11, 127.85, 129.48, 129.98, 130,16, 131,39, 142.68 (*C*=N), 178.54 (*C*=S). HRMS (ESI+): *m*/*z* calcd for $C_{16}H_{14}N_3S$ $(M+H)^+$ 280.0909, found 280.0919. ^{1}H NMR spectrum is in agreement with data reported in literature [69,70].

4.2. Enzyme preparation

The enzyme was isolated from mushrooms (*Agaricus bisporus*) purchased from a local supplier in Wrocław according to the procedure described by Gąsowska *et al*. [71] with slight modifications. The full description of enzyme preparation is included in electronic supplementary information.

4.3. Enzyme activity assay

The diphenolase activity of tyrosinase was checked using L-dopa as substrate. The activity assay was performed as described by Xie et al. [24] with slight modifications. Briefly, all investigated thiosemicarbazones were dissolved in DMSO and then diluted in 50 mM Na_2HPO_4-NaH_2PO_4 buffer (pH 6.8) to desired test concentrations (final concentration of DMSO in reaction mixture was below 1%). Enzyme solution (0.5 mg/ml, 40 000 U/mg) was diluted 5 times in 50 mM Na_2HPO_4-NaH_2PO_4 buffer (pH 6,8). 10 µl of diluted enzyme solution was first pre-incubated with the compounds in 50 mM Na_2HPO_4-NaH_2PO_4 buffer (pH 6.8) for 5 min at 25°C. After the solution of L-dopa was added the reaction was monitored by measuring the change in absorbance of colour product (dopachrome) for 5 min (λ = 475 nm, 25 °C) using Molecular Devices SpectraMax Plus 384 Microplate Reader. Control sample contained the same reagents as the test samples except for the substrate. Kojic acid was used as a positive control and was treated the same way as the other inhibitors.

4.4. Molecular docking

The structures of all the ligands were optimized in program Gaussian09 at the B3LYP/6-311g (d,p) level of theory [52] with the PCM solvent model using water as the solvent. Additionally, Merz-Singh-Kollman scheme [55] has been used for the determination of the atomic charges. The simulation of the docking process was performed using AutoDock v.4.2 program [54]. The starting geometry of the ligands as well as ligand charges has been assigned based on the *ab initio* calculations. The structure of tyrosinase was taken from the crystal structure of *Agaricus bisporus* deposited in Protein Data Bank [53]. Lacking protons and charges were added to the protein using H++ server [56, 57] according to pH value 6.8. During the docking process stereochemistry of C-N double bond has been fixed, whereas the rest of single bonds has been left as routable. The coordinates of the copper ions were taken as

a grid center in the docking process and the chosen grid had size 80x80x80 points. Each docking procedure using Lackmarkian Genetic Algorithm (LGA) was repeated until obtaining 200 conformations. Several possible structures of ligand-enzyme complex were gathered in the clusters for each type of ligand.

4.5. Cell proliferation assay

B16F10 cells were cultured in DMEM (Biowest) medium supplemented with 100 U/ml penicillin (Sigma-Aldrich), 100 U/ml streptomycin (Sigma-Aldrich) and 10% fetal bovine serum (Sigma-Aldrich). Cells were maintained in 5% CO_2 at 37°C.

Cells viability was estimated using colorimetric 3-(4,5-dimethylthiazol-2-yl)-2, 5-diphenyltetrazolium bromide (MTT) assay as described [72]. B16 cells were seeded into 96-well plate ($4x10^3$ cells/well) and incubated in the presence of tyrosinase inhibitors in various concentration (1000, 400, 100, 40, 10, 1, 0.1 μM) for 48 hours. As a control, DMSO and kojic acid were used. For the last 4 hours MTT was added into wells (0.625 mg/ml, Sigma-Aldrich). After that, lysing buffer was added in order to dissolve insoluble formazan. The absorbance was measured at 570 nm using Thermo Lab Multiscan RC microplate reader.

4.6. Measurement of melanin production

Measurement of melanin production in B16 cells was performed as described by Bellei *et al*. [72]. B16 cells were seeded into 96-well plate ($5x10^3$ cells/well) and stimulated with α-MSH (100 nM, Sigma-Aldrich). After 24 hours cells were treated with tyrosinase inhibitors as well as DMSO and kojic acid at a final concentration of 100, 40, 10, 4 and 1 μM. After 48 hours of incubation with inhibitors, cells were solubilized in 1N sodium hydroxide at 60°C for 2 hours. In order to measure melanin content, absorbance was measured at 405 nm using microplate reader.

Acknowledgements

The authors acknowledge the support from Wroclaw Centre of Biotechnology, programme The Leading National Research Center (KNOW) for years 2014-2018 and the Polish Ministry of Science and Higher Education (PMSHE) for the Faculty of Chemistry of Wrocław University of Science and Technology.

The molecular modeling was carried out using hardware and software resources of The Supercomputing and Networking Center in Wroclaw (grant no. 197).

References

[1] X. Lai, H.J. Wichers, M. Soler-Lopez, B.W. Dijkstra, Structure and Function of Human Tyrosinase and Tyrosinase-Related Proteins, Chem. Eur. J. 24 (2018) 47–55.

[2] P. Pongkai, T. Saisavoey, P. Sangtanoo, P. Sangvanich, A. Karnchanatat, Aphichart, Effects of protein hydrolysate from chicken feather meal on tyrosinase activity and melanin formation in B16F10 murine melanoma cells, Food Sci. Biotechnol. 26 (2018) 1199-1208.

[3] H. Hridya, A. Amrita, S. Mohan, M. Gopalakrishnan, T. K. Dakshinamurthy, G.P. Doss, R. Siva, Functionality study of santalin as tyrosinase inhibitor: A potential depigmentation agent, Int. J. Biol. Macromol. 86 (2016) 383–389.

[4] T. Pillaiyar, M. Manickam, V. Namasivayam, Skin whitening agents: medicinal chemistry perspective of tyrosinase inhibitors, J. Enzym. Inhib. Med. Ch. 32 (2017) 403-425.

[5] T. Pillaiyar, M. Manickamb, S.-H. Jung, Recent development of signaling pathways inhibitors of melanogenesis, Cellular Signalling 40 (2017) 99-115.
[6] H. Xu, X. Zhang, E. Karangwa, S. Xia, Correlating enzymatic browning inhibition and antioxidant ability of Maillard reaction products derived from different amino acids, J. Sci. Food Agric. 97 (2017) 4210-4218.
[7] M. Yusuf, P. Jain, Synthesis and biological significances of 1,3,4-thiadiazolines and related heterocyclic compounds, Arab. J. Chem. 7 (2014) 525-552.
[8] P. Chellan, S. Nasser, L. Vivas, K. Chibale, G.S. Smith, Cyclopalladated complexes containing tridentate thiosemicarbazone ligands of biological significance: Synthesis, structure and antimalarial activity, J. Organomet. Chem. 695 (2010) 2225-2232.
[9] H.C. Zhao, Y.P. Shi, Y.M. Liu, C.W. Li, L.N. Xuan, P. Wang, K. Zhang, B.Q. Chen, Synthesis and antitumor-evaluation of 1,3-selenazole-containing 1,3,4-thiadiazole derivatives, Bioorg. Med. Chem. Lett. 23 (2013) 6577-6579.
[10] Y. Yu , Y. Suryo Rahmanto, D.R. Richardson, Bp44mT: an orally active iron chelator of the thiosemicarbazone class with potent anti-tumour efficacy, Br. J. Pharmacol. 165 (2012) 148–166.
[11] M.-H. Yang, C.-M. Chen. Y.-H. Hu, C.-Y. Zheng, Z.-C. Li, L.-L. Ni, L. Sun, Q.-X. Chen, Inhibitory kinetics of DABT and DABPT as novel tyrosinase inhibitors, J. Biosci Bioeng. 115 (2013) 514-517.
[12] Z.-C. Li, L.-H. Chen, X.-J. Yu, Y.-H. Hu, K.K. Song, X.W. Zhou, Q.-X. Chen, Inhibition Kinetics of Chlorobenzaldehyde Thiosemicarbazones on Mushroom Tyrosinase, J. Agric. Food Chem. 58 (2010) 12537–12540.
[13]L.-H. Chen, Y.-H. Hu, W. Song, K.-K. Song, X. Liu, Y.-L. Jia, J.-X. Zhuang, Q.-X. Chen, Synthesis and Antityrosinase Mechanism of Benzaldehyde Thiosemicarbazones: Novel Tyrosinase Inhibitors, J. Agric.Food Chem. 60 (2012) 1542−1547.
[14] C.-B. Xue, L. Zhang, W.-C. Luo, X.-Y. Xie, L. Jiang, T. Xiao, 3D-QSAR and molecular docking studies of benzaldehyde thiosemicarbazone, benzaldehyde, benzoic acid, and their derivatives as phenoloxidase inhibitors, Bioorgan. Med. Chem. 15 (2007) 2006–2015.
[15] W. Yi, C. Dubois, S. Yahiaoui, R. Haudecoeur, C. Belle, H. Song, R. Hardré b, M. Réglier, A. Boumendjel, Refinement of arylthiosemicarbazone pharmacophore in inhibition of mushroom tyrosinase, Eur. J. Med. Chem. 46 (2011) 4330-4335.
[16] M.A. Soares, M.A. Almeida, C. Marins-Goulart, O.A. Chaves, A. Echevarria, M.C.C. de Oliveira, Thiosemicarbazones as inhibitors of tyrosinase enzyme, Bioorg. Med. Chem. Lett. 27 (2017) 3546-3550
[17] W. Yi, R.-H. Cao, Z.-Y. Chen, L. Yu, L. Ma, H.-C. Song, Design, Synthesis and Biological Evaluation of Hydroxy- or Methoxy-Substituted Phenylmethylenethiosemicarbazones as Tyrosinase Inhibitors, Chem. Pharm. Bull. 57 (2009) 1273-1277.
[18] W. Yi, R.-H. Cao, Z.-Y. Chen, L. Yu, H. Wen, Q. Yan, L. Ma, and H. Song, Rational Design and Synthesis of 4-*O*-Substituted Phenylmethylenethiosemicarbazones as Novel Tyrosinase Inhibitors, Chem. Pharm. Bull. 58 (2010) 752-754.
[19] A. You, J. Zhou, S. Song, G. Zhu, H. Song, W. Yi, Structure-based modification of 3-/4-aminoacetophenones giving a profound change of activity on tyrosinase: From potent activators to highly efficient inhibitors, European Journal of Medicinal Chemistry 93 (2015) 255-262.
[20] S. Song, A. You, Z. Chen, G. Zhu, H. Wen, H. Song, W. Yi, Study on the design, synthesis and structure-activity relationships of new thiosemicarbazone compounds as tyrosinase inhibitors, Eur. J. Med Chem. 139 (2017) 815-825.

[21] T.-H. Zhu, S.-W. Cao, Y.-Y. Yu, Synthesis, characterization and biological evaluation of paeonol thiosemicarbazone analogues as mushroom tyrosinase inhibitors, Int. J. Biol. Macromol. 62 (2013) 589-595.
[22] H. Dong, J. Liu, X. Liu, Y. Yu, S. Cao, Combining molecular docking and QSAR studies for modeling the anti-tyrosinase activity of aromatic heterocycle thiosemicarbazone analogues, J. Mol. Struct. 1151 (2018) 353-365.
[23] H. Dong, J. Liu, X. Liu, Y. Yu, S. Cao, Molecular docking and QSAR analyses of aromatic heterocycle thiosemicarbazone analogues for finding novel tyrosinase inhibitors, Bioorg. Chem. 75 (2017) 106–117.
[24] J. Xie, H. Dong, Y. Yu, S. Cao, Inhibitory effect of synthetic aromatic heterocycle thiosemicarbazone derivatives on mushroom tyrosinase: Insights from fluorescence, ^{1}H NMR titration and molecular docking studies, Food Chemistry 190 (2016) 709–716.
[25] J. Liu, M. Li, Y. Yu, S. Cao, Novel inhibitors of tyrosinase produced by the 4-substitution of TCT (Π), Int. J. Biol. Macromol. 103 (2017) 1096–1106.
[26] J. Xu, J. Liu, X. Zhu, Y. Yu, S. Cao, Novel inhibitors of tyrosinase produced by the 4-substitution of TCT, Food Chem. 221 (2017) 1530–1538.
[27] M.M. El-Sadek, S.Y. Hassan, H.E. Abdelwahab, G.A. Yacout, Synthesis of New 1,3,4-Thiadiazole and 1,2,3,4-Oxathiadiazole Derivatives from Carbohydrate Precursors and Study of Their Effect on Tyrosinase Enzyme, Molecules 17 (2012) 8378-8396.
[28] A. You, J. Zhou, S. Song, G. Zhu, H. Song, W. Yi, Rational design, synthesis and structure–activity relationships of 4-alkoxy- and 4-acyloxy-phenylethylenethiosemicarbazone analogues as novel tyrosinase inhibitors, Bioorganic & Medicinal Chemistry 23 (2015) 924–931.
[29] E. Buitrago, A. Vuillamy, A. Boumendjel, W. Yi, G. Gellon, R. Hardré, C. Philouze, G. Serratrice, H. Jamet, M. Regliér, C. Belle, Exploring the Interaction of N/S Compounds with a Dicopper Center: Tyrosinase Inhibition and Model Studies, Inorg. Chem. (2014), 53, 12848-12858.
[30] H. Arslan, N. Duran, G. Borekci, C.K. Ozer, C. Akbay, Antimicrobial Activity of Some Thiourea Derivatives and Their Nickel and Copper Complexes, Molecules 14 (2009) 519-527.
[31] S. Parvez, M. Kang, H.-S. Chung, H. Bae, Naturally Occurring Tyrosinase Inhibitors: Mechanism and Applications in Skin Health, Cosmetics and Agriculture Industries Phytother. Res. 21 (2007) 805–816.
[32] Y.J. Kima, H. Uyamab, Tyrosinase inhibitors from natural and synthetic sources: structure, inhibition mechanism and perspective for the future, Cell. Mol. Life Sci. 62 (2005) 1707-1723.
[33] M. Serda, J.G. Małecki, A. Mrozek-Wilkiewicz, R. Musioł, J. Polański, Microwave assisted synthesis, X-ray crystallography and DFT calculationsof selected aromatic thiosemicarbazones, J. Mol. Struct. 1037 (2013) 63–72.
[34] T.K. Venkatachalam, G.K. Pierens, D.C. Reutens, Synthesis, NMR structural characterization and molecular modeling of substituted thiosemicarbazones and semicarbazones using DFT calculations to prove the syn/anti isomer formation, Magn. Reson. Chem. 52 (2014) 98–105.
[35] J. Song, L.M. Jones, G.D. Kishore Kumar, E.S. Conner, L. Bayeh, G.E. Chavarria, A.K. Charlton-Sevcik, S.-E. Chen, D.J. Chaplin, M.L. Trawick, K.G. Pinney, Synthesis and Biochemical Evaluation of Thiochromanone Thiosemicarbazone Analogues as Inhibitors of Cathepsin LACS, Med. Chem. Lett. 3 (2012) 450−453.
[36] P. Makam, R. Kankanala, A. Prakash, T. Kannan, 2-(2-Hydrazinyl)thiazole derivatives: Design, synthesis and in vitro antimycobacterial studies, Eur. J. Med. Chem. 69 (2013) 564-576.

[37] P.V. Bernhardt, M. Martínez, C. Rodríguez, M. Vazquez, Biologically active thiosemicarbazone Fe chelators and their reactions with ferrioxamine B and ferric EDTA; a kinetic study, Dalton Trans. 41 (2012) 2122-2130.
[38] T.K. Venkatachalam, P.V. Bernhardt, C.J. Noble, N. Fletcher, G.K. Pierens, K.J. Thurecht, D.C. Reutens, Synthesis, characterization and biological activities of semicarbazones and their copper complexes, J. Inorg. Biochem. 162 (2016) 295–308.
[39] L.A. Lessa, D.C. Reis, J.G. Da Silva, L.T. Paradizzi, N.F. da Silva, Mde F Carvalho, S.A. Siqueira, H. Beraldo, Coordination of Thiosemicarbazones and Bis(thiosemicarbazones) to Bismuth(III) as a Strategy for the Design of Metal-Based Antibacterial Agents, Chem. Biodivers. 9 (2012) 1955-1966.
[40] O. Dömötör, N.V. May, K. Pelivan, T. Kiss, B.K. Keppler, C.R. Kowol, É. A. Enyedy, A comparative study of α-N-pyridyl thiosemicarbazones: Spectroscopic properties, solution stability and copper(II) complexation, Inorganica Chim. Acta 472 (2018) 264–275.
[41] D.R. Richardson, D.S. Kalinowski, V. Richardson, P.C. Sharpe, D.B. Lovejoy, M. Islam, P.V. Bernhardt, 2-Acetylpyridine Thiosemicarbazones are Potent Iron Chelators and Antiproliferative Agents: Redox Activity, Iron Complexation and Characterization of their Antitumor Activity, J. Med. Chem. 52 (2009) 1459–1470.
[42] V. Opletalová, D.S. Kalinowski, M. Vejsová, J. Kuneš, M. Pour, J. Jampílek, V. Buchta, D.S. Richardson, Identification and Characterization of Thiosemicarbazones with Antifungal and Antitumor Effects: Cellular Iron Chelation Mediating Cytotoxic, Activity Chem. Res. Toxicol. 21 (2008) 1878–1889.
[43] A.A. Ali, H. Nimir, C. Aktas, V. Huch, U. Rauch, K.H. Schäfer, M. Veith, Organoplatinum(II) Complexes with 2-Acetylthiophene Thiosemicarbazone: Synthesis, Characterization, Crystal Structures, and in Vitro Antitumor Activity, Organometallics 31 (2012) 2256−2262.
[44] H.R. Fatondji, S. Kpoviessi, F. Gbaguidi, J. Bero, V. Hannaert, J. Quetin-Leclercq, J. Poupaert, M. Moudachirou, G.C Accrombessi, Structure–activity relationship study of thiosemicarbazones on an African trypanosome: Trypanosoma brucei brucei, Med. Chem. Res. 22 (2013) 2151–2162.
[45] P. Thanigaimalai, K.C. Lee, V.K. Sharma, E. Roh, Y. Kim, S.H. Jung, Ketonethiosemicarbazones: Structure–activity relationships for their melanogenesis inhibition Bioorganic Med. Chem. Lett. 21 (2011) 3527–3530.
[46] C. Murakata, Y. Yamashita, R. Nakai, K. Akasaka, Y. Ino, K. Kato, Y. Kitamura, M-stage Kinesin inhibitor, *European Patent Application* EP616866 **2006** (see page 65)].
[47] J.R. Dimmock, J.M. McColl, S.L. Wonko, R.S. Thayer, D.S. Hancock, Evaluation of the thiosemicarbazones of some aryl alkyl ketones and related compounds for anticonvulsant activities, Eur. J. Med. Chem. 26 (1991) 529-534.
[48] K. Bagherzadeh, F.S. Talari, A. Sharifi, M.R. Ganjali, A.A. Saboury, M. Amanlou, A new insight into mushroom tyrosinase inhibitors: docking, pharmacophore-based virtual screening, and molecular modeling studies, J. Biomol. Struct. Dyn. 33 (2015) 487–501.
[49] T.-S. Chang, An Updated Review of Tyrosinase Inhibitors, Int. J. Mol. Sci. 10, (2009), 2440-2475.
[50] J.S. Chen , C.I. Wei, M. R. Marshall, Inhibition mechanism of kojic acid on polyphenol oxidase, J. Agric. Food Chem. 39 (1991) 1897–1901.
[51] R.A Copeland, Enzymes: A Practical Introduction to Structure, Mechanism, and Data Analysis, second ed., Viley-VCH, New York, 2000.
[52] Gaussian 09, Revision D.01, M. J. Frisch, G. W. Trucks, H. B. Schlegel, G. E. Scuseria, M. A. Robb, J. R. Cheeseman, G. Scalmani, V. Barone, B. Mennucci, G. A. Petersson, H. Nakatsuji, M. Caricato, X. Li, H. P. Hratchian, A. F. Izmaylov, J. Bloino, G. Zheng, J. L. Sonnenberg, M. Hada, M. Ehara, K. Toyota, R. Fukuda, J. Hasegawa, M. Ishida, T. Nakajima,

Y. Honda, O. Kitao, H. Nakai, T. Vreven, J. A. Montgomery, Jr., J. E. Peralta, F. Ogliaro, M. Bearpark, J. J. Heyd, E. Brothers, K. N. Kudin, V. N. Staroverov, T. Keith, R. Kobayashi, J. Normand, K. Raghavachari, A. Rendell, J. C. Burant, S. S. Iyengar, J. Tomasi, M. Cossi, N. Rega, J. M. Millam, M. Klene, J. E. Knox, J. B. Cross, V. Bakken, C. Adamo, J. Jaramillo, R. Gomperts, R. E. Stratmann, O. Yazyev, A. J. Austin, R. Cammi, C. Pomelli, J. W. Ochterski, R. L. Martin, K. Morokuma, V. G. Zakrzewski, G. A. Voth, P. Salvador, J. J. Dannenberg, S. Dapprich, A. D. Daniels, O. Farkas, J. B. Foresman, J. V. Ortiz, J. Cioslowski, D. J. Fox, Gaussian, Inc., Wallingford CT, 2013.

[53] W.T. Ismaya, H.J. Rozeboom, A. Weijn, F. Fusetti, H.J. Wichers, B.W. Dijkstra, Crystal structure of Agaricus bisporus mushroom tyrosinase: identity of the tetramer subunits and interaction with tropolone, Biochemistry 50 (2011) 5477-5486.

[54] G. M. Morris, R. Huey, W. Lindstrom, M.F. Sanner, R.K. Belew, D.S Goodsell, A.J. Olson, Autodock4 and AutoDockTools4: automated docking with selective receptor flexibility, J. Comput. Chem. 16 (2009) 2785-2791.

[55]B. H. Besler, K. M. Merz Jr., P. A. Kollman, Atomic charges derived from semiempirical methods, J. Comput. Chem. 11 (1990) 431-439.

[56] http://biophysics.cs.vt.edu/H++

[57] R. Anandakrishnan, B. Aguilar, A.V. Onufriev, H++ 3.0: automating pK prediction and the preparation of biomolecular structures for atomistic molecular modeling and simulation, Nucleic Acids Res. 40 (2012) 537-541.

[58]T.-S. Chang, Natural Melanogenesis Inhibitors Acting Through the Down-Regulation of Tyrosinase Activity, Materials, 5 (2012) 1661-1685.

[59] A. Lehraiki, P. Abbe, M. Cerezo, F. Rouaud, C. Regazzetti, B. Chignon-Sicard, T. Passeron, C. Bertolotto, R. Ballotti, S. Rocchi, Inhibition of Melanogenesis by the Antidiabetic Metformin, J. Invest. Dermatol. 134 (2014) 2589-2597.

[60] N. Sun, B. Li, J.P. Shao, W.M. Mo, B.X. Hu, Z.L. Shen, X.Q. Hu, A general and facile one-pot process of isothiocyanates from amines under aqueous conditions, Beilstein J. Org. Chem. 8 (2012) 61-70.

[61] B. Hu, B. Wang, B. Zhao, Q. Guo, Z.H. Li, X.H. Zhang, G.Y. Liu, Y. Liu, Y. Tang, F. Luo, Y. Du, Y.X. Chen, L.Y. Ma, H.M. Liu, Thiosemicarbazone-based selective proliferation inactivators inhibit gastric cancer cell growth, invasion, and migration, Med. Chem. Commun. 8 (2017) 2173-2180.

[62] S.J. Yang, J.H. Choe, Y.D. Gong, Solid-Phase Synthesis of 1,3,4-Thiadiazole Derivatives via Desulfurative Cyclization of Thiosemicarbazide Intermediate Resin, *ACS Comb. Sci.* 18 (2016) 499–506.

[63] A.R. Katritzky, N.M. Khashab, A.V. Gromova, Preparations of diversely substituted thiosemicarbazides and N-hydroxythioureas, Arkivoc 3 (2006) 226-236.

[64] A.G. Mal'kina, V.V Nosyreva, A.I. Albanov, A.V. Afonin, A.V. Vashchenko, S.V. Amosova, B.A. Trofimov, Regioselective N(2)-H-functionalization of thiosemicarbazones of aromatic and heteroaromatic aldehydes with acrylonitrile Synth. Commun. 47 (2017) 159–168.

[65] K.H. Markiewicz, P. Zembko, K. Półtorak, I. Misztalewska, S. Wojtulewski, A.M. Majcher, E. Fornal, A.Z. Wilczewska, Magnetic nanoparticles with chelating shells prepared by RAFT/MADIX polymerization, New J. Chem. 40 (2016) 9223-9231.

[66] L. Blau, R.F. Menegon, G.H.G. Trossini, J.V.D. Molino, D.G. Vital, R.M.B. Cicarelli, G.D. Passerini, P.L. Bosquesi, C.M. Chin, Design, synthesis and biological evaluation of new aryl thiosemicarbazone as antichagasic candidates, Eur. J. Med. Chem. 67 (2013) 142-151.

[67] X.H. Du, C. Guo, E. Hansell, P.S. Doyle, C.R. Caffrey, T.P. Holler, J.H. McKerrow, F.E. Cohen, Synthesis and Structure−Activity Relationship Study of Potent Trypanocidal Thio

Semicarbazone Inhibitors of the Trypanosomal Cysteine Protease Cruzain, J. Med. Chem. 45 (2002) 2695–2707.
[68] G. D. K. Kumar, G.E. Chavarria, A.K. Charlton-Sevcik, G.K. Yoo, J. Song, T.E. Strecker, B.G. Siim, D.J. Chaplin, M.L. Trawicka, G.K. Pinneya, Functionalized benzophenone, thiophene, pyridine, and fluorene thiosemicarbazone derivatives as inhibitors of cathepsin L G, Bioorganic Med. Chem. Lett. 20 (2010) 6610-6615.
[69] J. Bai, R..H. Wang, Y. Qiao, A. Wang, C.J. Fang, Schiff base derived from thiosemicarbazone and anthracene showed high potential in overcoming multidrug resistance in vitro with low drug resistance index, Drug Des Devel Ther. 11 (2017) 2227–2237.
[70] I.E. Tolpygin, Thiosemicarbazones as Effective Fluorescent Sensors for Cations and Anions Russ. J. Gen. Chem. 82 (2012) 1533–1536.
[71] B. Gąsowska, P. Kafarski, H. Wojtasek, Interaction of mushroom tyrosinase with aromatic amines, o-diamines and o-aminophenols, BBA-Gen Subjects 1673 (2004) 170-177.
[72] B. Bellei , A. Pitisci, E. Izzo, M. Picardo, Inhibition of Melanogenesis by the Pyridinyl Imidazole Class of Compounds: Possible Involvement of the Wnt/β-Catenin Signaling Pathway, PLoS ONE 7 (2012) e33021.

Highlights

- Thiosemicarbazones can be considered as potent tyrosinase inhibitors
- Small groups on thiosemicarbazone skeleton are preferable for tyrosinase inhibition
- Thiosemicarbazones reveals very well inhibitory activity against melanogenesis

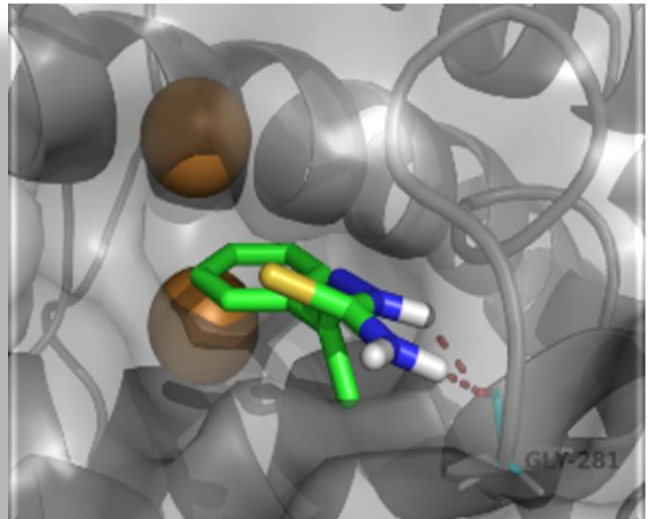

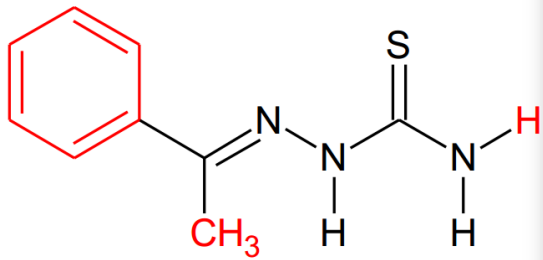

K_i = 0.38 µM

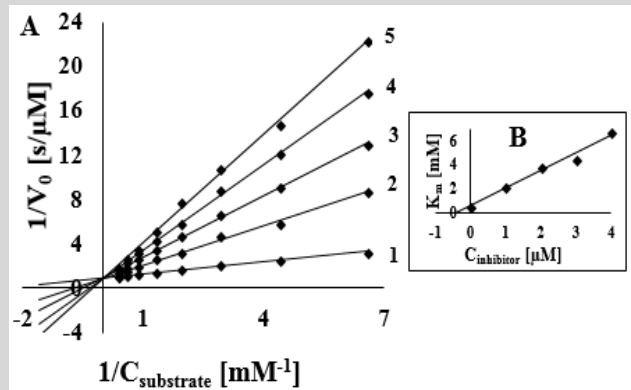

Favourable arrangement of **substituents** on thiosemicarbazone skeleton for inhibition of mushroom tyrosinase.